

4 × 4 wavelength-reconfigurable photonic switch based on thermally tuned silicon microring resonators

Han-Yong Ng

Michael R. Wang, MEMBER SPIE

University of Miami
Department of Electrical
and Computer Engineering
Coral Gables, Florida 33124
E-mail: mwang@miami.edu

Daqun Li

New Span Opto-Technology, Inc.
16115 SW 117 Avenue, A-15
Miami, Florida 33177

Xuan Wang

Jose Martinez

Roberto R. Panepucci, MEMBER SPIE

Florida International University
Department of Electrical
and Computer Engineering
Miami, Florida 33174

Kachesh Pathak

U.S. Army Space & Missile Defense
Command
Huntsville, Alabama 35807

Abstract. Microring resonators (MRs) are important photonic devices for large-port-count photonic circuits owing to their micrometer-scale device sizes. We describe the implementation of a 4 × 4 wavelength-reconfigurable photonic switch consisting of eight tunable MRs fabricated on a less expensive material platform: silicon on insulator. Wavelength reconfiguration is achieved through independent thermo-optic tuning of MRs with localized Nichrome microheaters fabricated on the same silicon-on-insulator substrate. A free spectral range of 18 nm and a 3-dB linewidth of 0.1 nm were observed for the fabricated MRs with a diameter of approximately 10 μm. The switch device shows negligible channel crosstalk (<0.01 nm) and moderate switching response time (<1 ms). The switch can potentially be scaled up to benefit the development of large-scale integrated photonics. © 2008 Society of Photo-Optical Instrumentation Engineers. [DOI: 10.1117/1.2909662]

Subject terms: microring resonator; photonic switch; thermo-optic tuning; silicon.

Paper 070853R received Oct. 16, 2007; revised manuscript received Jan. 16, 2008; accepted for publication Jan. 26, 2008; published online Apr. 28, 2008.

1 Introduction

Optical switches are essential elements in optical networks and optical communication systems as conventional electrical-optical and optical-electrical communication networks are being replaced with all-optical ones to meet the ever-increasing capacity demand in both traffic volume and bandwidth. This has called for the development of a variety of photonic devices with high port counts, and optical switches are one of the most important elements in this category. To achieve high port counts on a small footprint, highly integrated photonic devices have to be developed.

Microring resonators (MRs) are well-known photonic devices that offer a promising solution to high-port-count optical switching applications owing to their micrometer-scale device sizes. They have been widely employed as wavelength add-drop filters¹ and wavelength-division multiplexers and demultiplexers.² MR fabrication requires high refractive index contrast (~3.5 : 1.5) between the guiding material and the cladding layers to achieve strong optical confinement in small bending radius. For this reason, both III-V compounds³ and silicon-on-insulator (SOI) material⁴ have been used for MR fabrication.

To facilitate a wavelength-reconfigurable photonic switch with MRs, the MRs must be tunable. So far, thermo-optic and electro-optic tuning methods have been demonstrated.^{5,6} Compared to electro-optic tunable MRs, MRs tuned by thermo-optic means demand less complex device layer structure and consequently yield easier fabrication steps. While thermo-optic tuning of a single MR is readily achievable, independent thermo-optic tuning of multiple MRs fabricated on the same substrate is more challenging, especially when these MRs are fabricated closely on a highly integrated photonic circuit.

We have developed a 1 × 4 wavelength-reconfigurable photonic switch using thermally tuned MRs fabricated on a SOI substrate.⁷ In this paper, we describe our continuing development of a MR-based 4 × 4 photonic switch capable of independent wavelength tuning through localized microheaters implemented on the same SOI substrate. Device design and fabrications are described, and then the fabricated photonic switch is fully characterized. Finally, future performance improvements of the fabricated 4 × 4 photonic switch are discussed.

2 Design and Fabrication

As illustrated in Fig. 1, the waveguide structure of the 4 × 4 photonic switch device consists of eight MRs (four

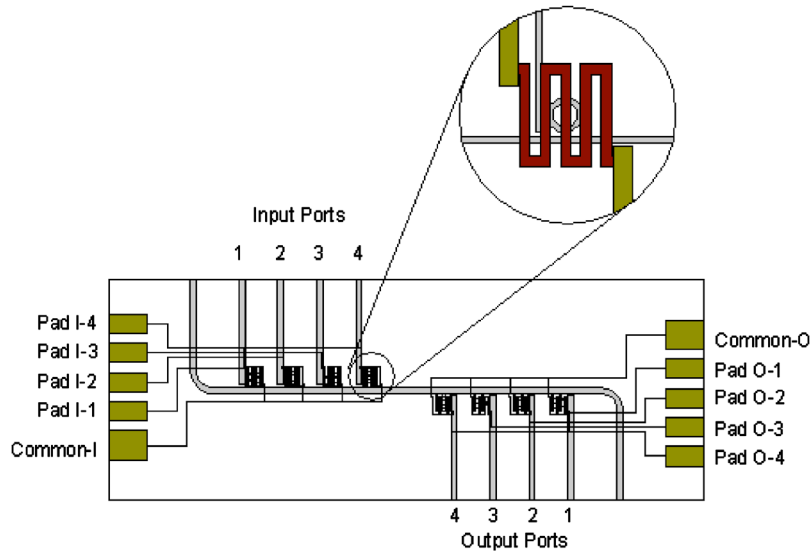


Fig. 1 Schematic of the 4×4 wavelength reconfigurable photonic switch with MRs and local micro-heaters, shown in an enlarged view (inset).

each on the input and output sides), eight straight port waveguides, and a main throughput waveguide. Due to device symmetry, the input and output ports are interchangeable. With this configuration, the main waveguide combines all four input channel signals that are wavelength-selected by the input MRs, by means of evanescent coupling. These four signals are then selectively routed to the corresponding output ports by the output MRs in a similar manner. A routing path from input end to output end is formed when an input MR and an output MR are tuned to a matched resonance wavelength. The main waveguide, the straight add-drop port waveguides, and the ring waveguides forming the MRs are designed with a uniform height and width of 250 and 450 nm, respectively, for single-mode operation around 1550-nm wavelength. All MRs are de-

signed with an equal diameter of 10 μm, yielding a free spectral range (FSR) of approximately 17.6 nm at 1550-nm wavelength according to

$$FSR = \frac{\lambda^2}{2\pi r n_g}, \quad (1)$$

where λ is the resonant wavelength of the MR, n_g is the MR group index of refraction (~4.35),⁸ and r is the MR radius. The lateral separation gap between a MR and its adjacent add-drop port as well as the main waveguide is 250 nm. To facilitate standard fiber array connection, adjacent waveguide ports on both input and output sides are spaced at 250 μm. We designate input and output sides for easier reference. The device can operate bidirectionally.

The 4×4 photonic switch device was fabricated on an SOI wafer with a 3-μm-thick buried oxide layer. We chose

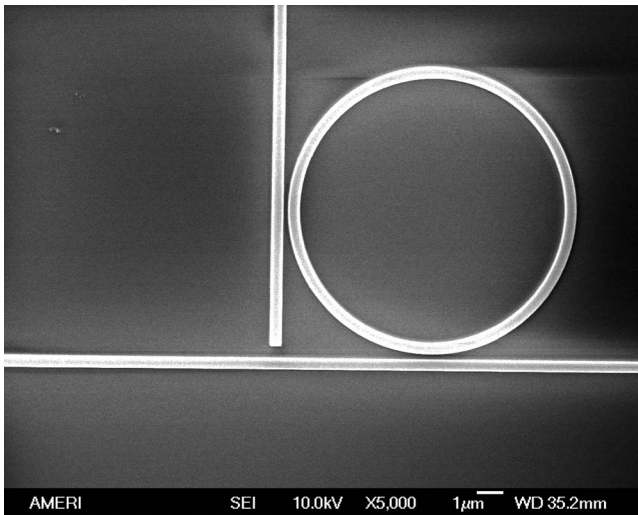


Fig. 2 Local SEM image of a MR with coupling waveguides, main waveguide (horizontal), and add-drop port waveguide (vertical).

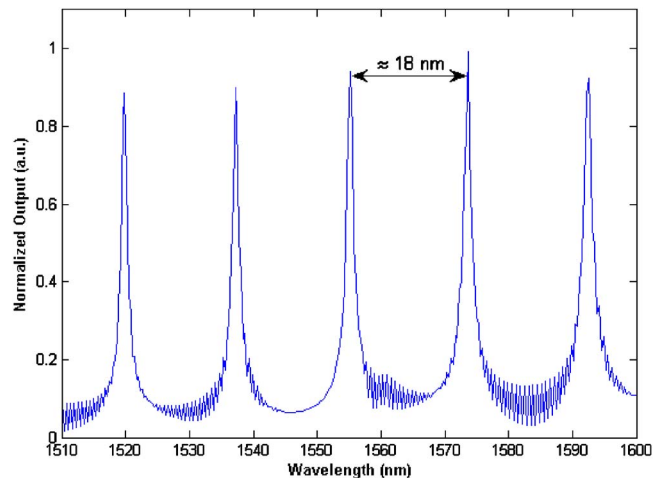


Fig. 3 FDTD simulation of a MR 10 μm in diameter, showing the expected FSR at 1550 nm.

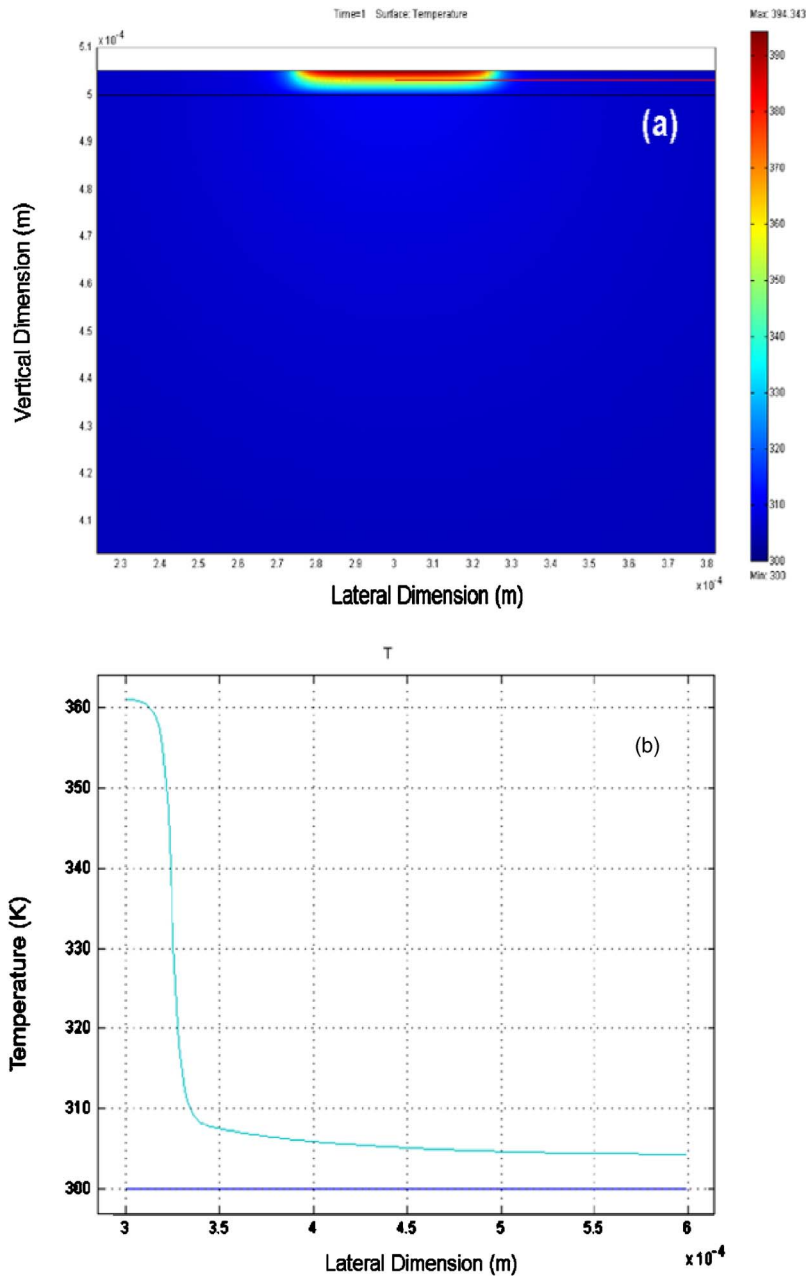


Fig. 4 FEM thermal simulation of temperature distribution around a microheater on SiO₂ layer (a), and temperature variation as a function of the horizontal distance from the center of a microheater (b).

the laterally coupled scheme to simplify the device fabrication and to facilitate localized thermal tuning. Our device fabrication procedures are similar to those commonly used in the fabrication of silicon micro-electronics. First, FOX 12 photoresist from Dow Corning was spun on the SOI substrate at 2000 rpm, and then the wafer was baked for 2 min at 200°C. Pattern exposure was done on a Leica VB6 e-beam system at 100 kV with 1-nA current and a beam step size of 5 nm. The exposed wafer was developed in a MIF300 developer for 2 min, and waveguides were formed through inductively coupled plasma etching with a Plasma Therm etcher (770 ICP). A chlorine-argon plasma mixture was used as the etching recipe. The etching time was 90 s, with 20% overetch to obtain verticality and

smoothness of waveguide sidewalls. As a final silicon fabrication step, a 1- μm -thick cladding layer of SiO₂ was coated by plasma-enhanced chemical vapor deposition. To achieve MR thermo-optic tuning, Nichrome resistive microheaters in a zigzag shape (Fig. 1 inset) were layered on the top cladding layer directly above each MR. The microheaters have a linewidth of 5 μm and a thickness of 0.1 μm , and cover an area of 50 × 50 μm^2 per heater immediately above their respective MR. The resistance of each microheater is estimated to be around 900 Ω (Nichrome resistivity $\sim 1.50 \times 10^{-6} \Omega \text{ m}$ at room temperature). Finally, low-resistance Ti-Au wires and electrode pads were evaporated on top to guide heating currents to the MRs. Due to the lower resistivity of $2.44 \times 10^{-8} \Omega \text{ m}$ for these

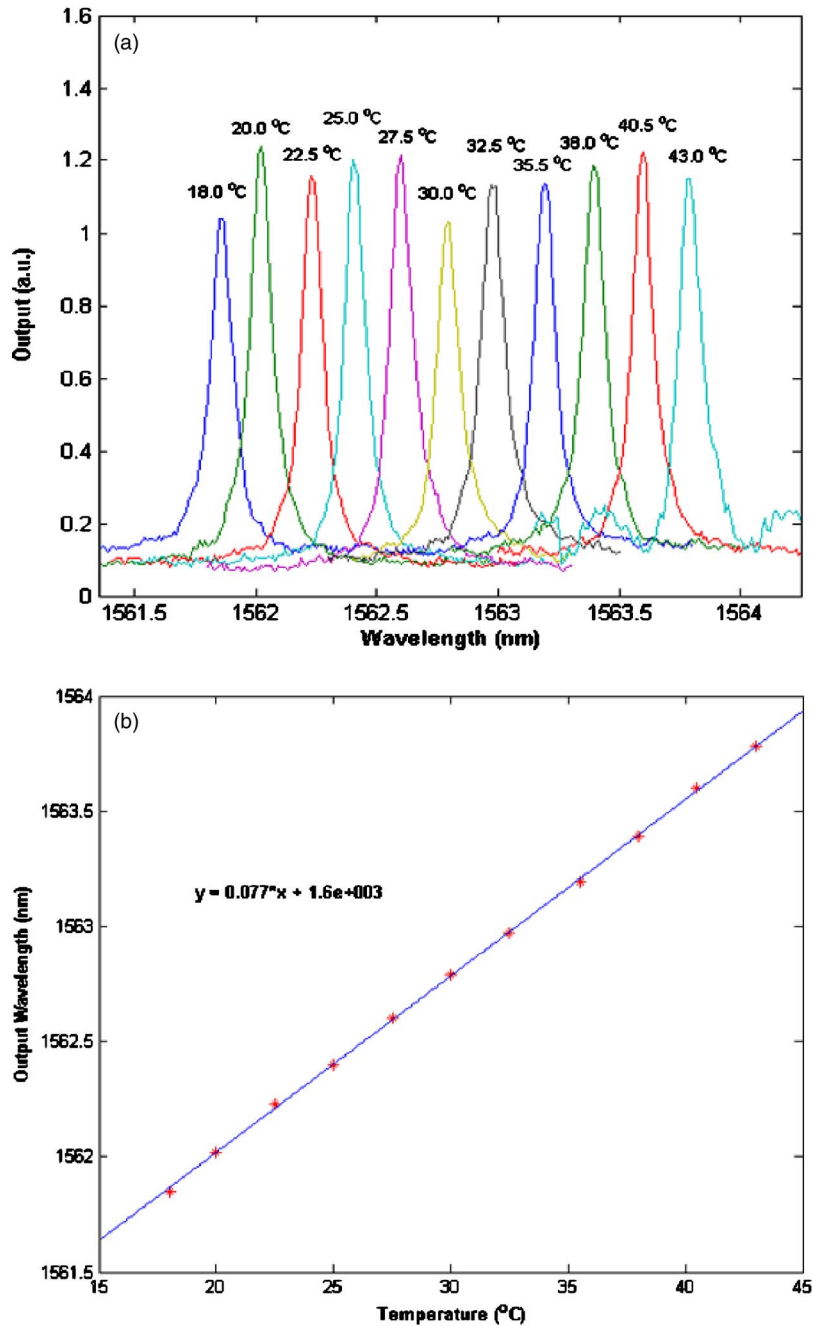


Fig. 5 Resonant spectrum of a MR at various temperatures (a), and relationship between MR resonant wavelength peak and MR temperature (b).

conductive wires, the resistance of each pair of wires forming the current loop is estimated to be about 13.5Ω . This indicates that more than 98% of the heating power supplied to a microheater through the current loop is effectively dissipated in the heating area.

Figure 2 presents a scanning electron microscopic (SEM) image of a fabricated MR and its adjacent coupling waveguides, taken before the deposition of the heating elements. The figure shows clearly the 250-nm separation gap between the MR and its adjacent waveguides.

To verify our device design, we conducted simulations of both the MR and the microheater. Figure 3 shows the

normalized spectral profile of a MR, with a $10\text{-}\mu\text{m}$ diameter, in a three-dimensional finite-difference time domain (FDTD) using waveguide simulation software from RSoft[®] for the transverse electric (TE) polarization mode. A FSR of 18 nm around 1550-nm wavelength is confirmed in this figure.

The heat dissipation of a microheater was studied using the finite-element method (FEM) simulation software (FEMLAB[®]) in cylindrical device symmetry, as seen in Fig. 4(a). It was found that an electric intensity level of $26 \text{ mW}/\mu\text{m}^2$ (equivalent to $\sim 9\text{-mA}$ heating current) is

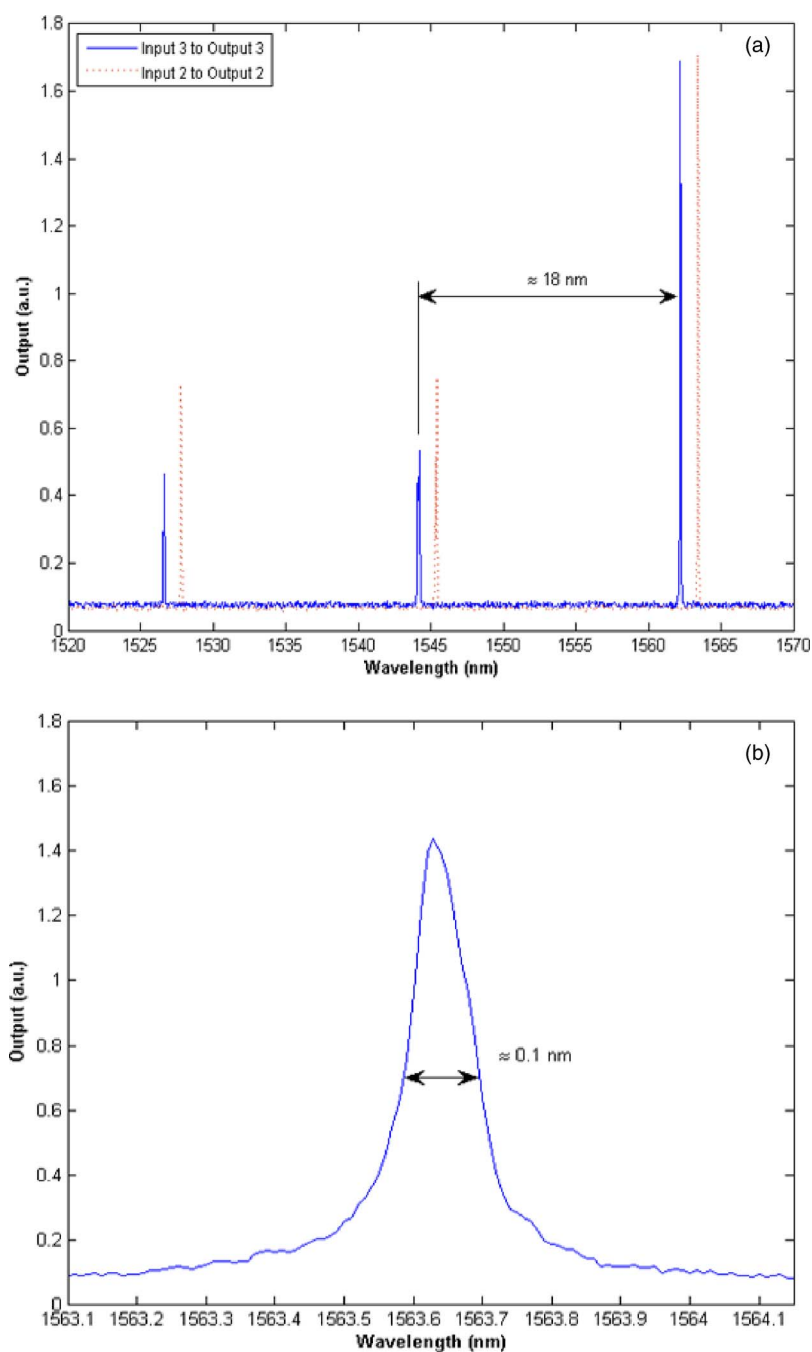


Fig. 6 Spectral profile of a MR showing a FSR of approximately 18 nm at 1550 nm (a), and a resonant spectral curve of a MR revealing a FWHM of roughly 0.1 nm (b).

needed to increase the local temperature by 60°C . Assuming an ideal heat transfer to the MR with no temperature gradient between the microheater and the MR, this current level would tune the MR by about 5 nm. The three-dimensional axially symmetric simulation also confirms highly vertical heat penetration through the top cladding SiO_2 layer to reach the MR beneath with little horizontal spreading. Figure 4(b) shows the simulated temperature profile versus horizontal distance from the center of a microheater at a depth of $2\ \mu\text{m}$ from the top surface. As in-

dicated in Fig. 4(b), the heating was found to remain highly localized with negligible thermal effect on adjacent MRs located $250\ \mu\text{m}$ away.

3 Device Characterization

To eliminate the effect of ambient temperature fluctuations on the device, a Peltier thermoelectric cooler (TEC) was mounted at the back of the device substrate with device temperature stabilized at $(22 \pm 0.01)^{\circ}\text{C}$. A tunable laser

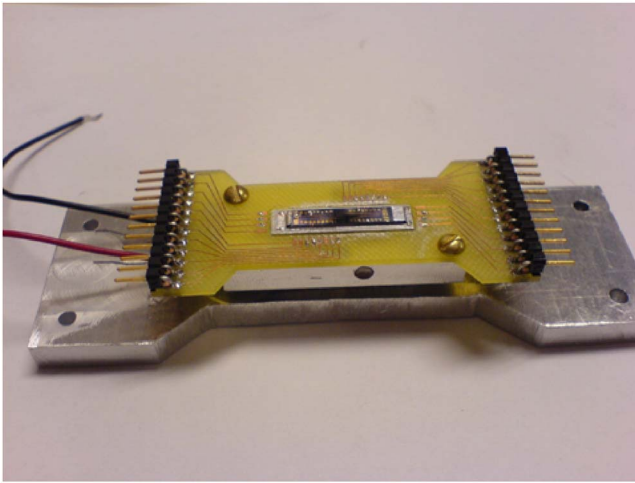


Fig. 7 Picture of the TEC temperature-regulated switch device and PCB assembly.

Table 1 Resonant wavelength peaks of the MRs and the resistances of their corresponding microheaters

| MR | Resonant wavelength (nm) | Microheater resistance (Ω) |
|----------|--------------------------|-------------------------------------|
| Input 1 | 1561.29 | 963 |
| Input 2 | 1561.51 | 1029 |
| Input 3 | 1561.11 | 1045 |
| Input 4 | 1561.71 | 970 |
| Output 1 | 1561.99 | 782 |
| Output 2 | 1561.48 | 607 |
| Output 3 | 1561.30 | 868 |
| Output 4 | 1561.60 | 784 |

(Photonics, Tunics-BT) with a wavelength step size of 0.01 nm was used for device characterization. The laser source was butt-coupled to an input waveguide port of the device using a polarization-maintaining (PM) fiber to preserve the required TE polarization, since our device was designed for TE polarization mode. A microscope objective lens was used to couple the light emitted from the output ports of the device to a photodetector (Agilent, 81626B). To remove optical noise signals caused by substrate leakage, an adjustable iris diaphragm acting as a spatial optical filter was placed between the objective lens and the photodetector. The analog output of the photodetector was then digi-

tized by a computer that also ran a LabVIEW® program designed to scan the wavelength of the laser source.

The thermal tuning coefficient of a MR was evaluated by varying the temperature of the entire device through the TEC while monitoring the resonant wavelength peak of a MR. To facilitate the global tuning with the TEC, the main waveguide was used as the input port to bypass any input MRs, so that only a single output MR was contained in the routing path from input to output. As a result, the thermo-optic tuning characteristic of a single MR can be revealed, as seen in Fig. 5(a). As expected, Fig. 5(b) shows a linear

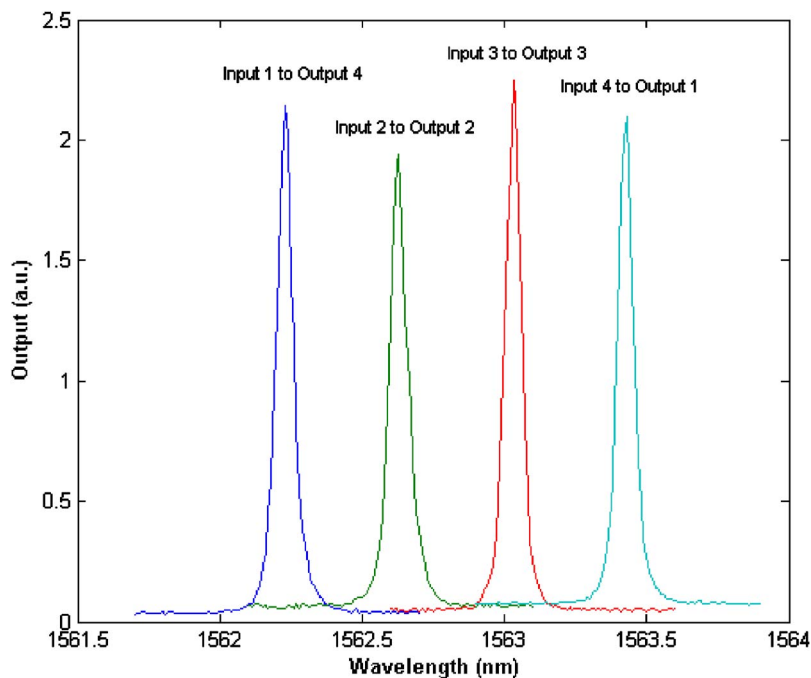


Fig. 8 One switching configuration of the 4 × 4 photonic switch with λ_1 , λ_2 , λ_3 , and λ_4 routed from input ports 1, 2, 3, and 4 to output ports 4, 2, 3, and 1, respectively.

Table 2 Heating currents determined to tune the MRs to the corresponding wavelength channels, with the current set marked in bold for the switching configuration shown in Fig. 8.

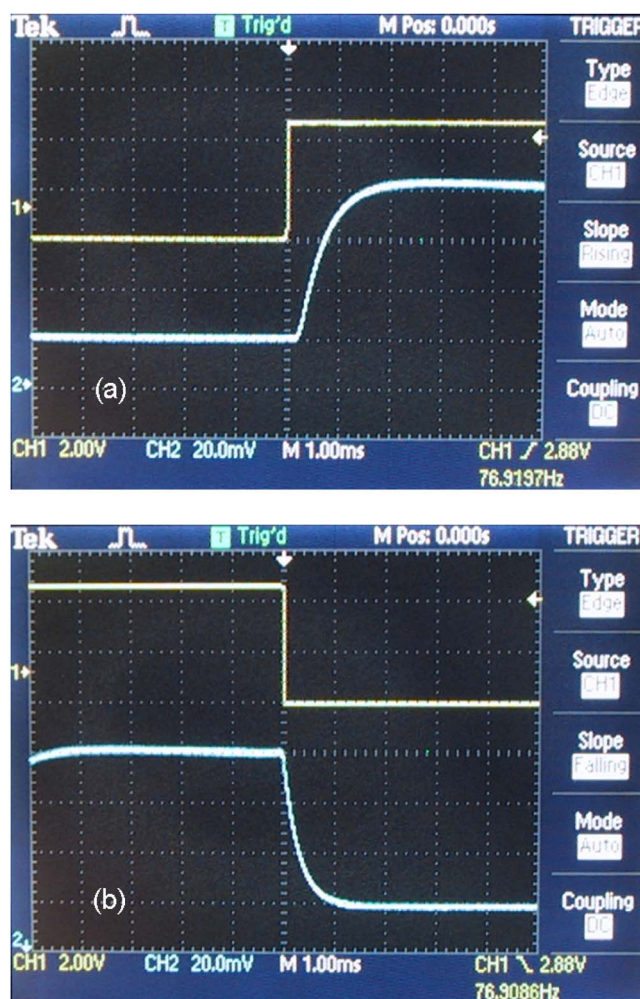
| | Heating current (mA) | | | |
|-------------------------------|-----------------------------|-----------------------------|-----------------------------|-----------------------------|
| | λ_1 (1562.23 nm) | λ_2 (1562.63 nm) | λ_3 (1563.03 nm) | λ_4 (1563.43 nm) |
| Input port 1 (I-MR 1) | 4.40 | 5.21 | 6.00 | 6.59 |
| Input port 2 (I-MR 2) | 4.14 | 5.09 | 5.83 | 6.48 |
| Input port 3 (I-MR 3) | 4.27 | 5.05 | 5.74 | 6.30 |
| Input port 4 (I-MR 4) | 3.12 | 4.28 | 5.13 | 5.87 |
| Output port 1 (O-MR 1) | 2.25 | 3.73 | 4.71 | 5.58 |
| Output port 2 (O-MR 2) | 3.75 | 4.72 | 5.57 | 6.19 |
| Output port 3 (O-MR 3) | 4.47 | 5.38 | 6.18 | 6.83 |
| Output port 4 (O-MR 4) | 3.76 | 4.75 | 5.56 | 6.36 |

relationship between the resonant wavelength peak of the MR and its temperature, yielding a thermal tuning coefficient of approximately 0.08 nm/K for the MR.

The FSR of the MRs was measured by scanning the laser source from 1520 to 1580 nm with a step size of 0.05 nm while monitoring the output spectrum of the MR. The device temperature was kept constant at $(22 \pm 0.01)^\circ\text{C}$ by the TEC to eliminate any resonant wavelength shift caused by room temperature variations. As shown in Fig. 6(a), a FSR of approximately 18 nm was observed for the MR around 1550-nm wavelength, which is very close to our FDTD simulation result. To resolve the spectral profile of the MR, the resonant spectral profile of a MR was acquired using a smaller wavelength step size of 0.01 nm, and a full width at half maximum (FWHM) of about 0.1 nm was observed as seen in Fig. 6(b). Although all MRs are designed to have the same diameter, there is a difference of 1 nm in resonant peak wavelength among the fabricated MRs, due to their size variations caused by fabrication non-uniformities. This translates into approximately 6.5-nm variations in the actual diameter among the fabricated MRs.

To implement local thermo-optic tuning of MRs with microheaters, a printed circuit board (PCB) was fabricated with electric wires bonded to the electrode pads on the switch device. Thermal silver epoxy was used to bond fine stripped magnet wires with a diameter of $45\ \mu\text{m}$ to the PCB and the electrode pads on the device. Figure 7 shows a photograph of the TEC-controlled switch device and the PCB assembly. The resonant wavelength peaks of the eight MRs and the resistances of their corresponding microheaters are presented in Table 1. For this 4×4 photonic switch, the following four ITU grids were chosen as the wavelength channels: $\lambda_1 = 1562.23\ \text{nm}$, $\lambda_2 = 1562.63\ \text{nm}$, $\lambda_3 = 1563.03\ \text{nm}$, and $\lambda_4 = 1563.43\ \text{nm}$. As a result, there are a total of $4! \times 4! = 576$ switching configurations.

Figure 8 shows one switching configuration with input 1 and output 4, input 2 and output 2, input 3 and output 3,

**Fig. 9** Tuning response time of the switch device, showing the turn-on time delay (a) and the turn-off time delay (b).

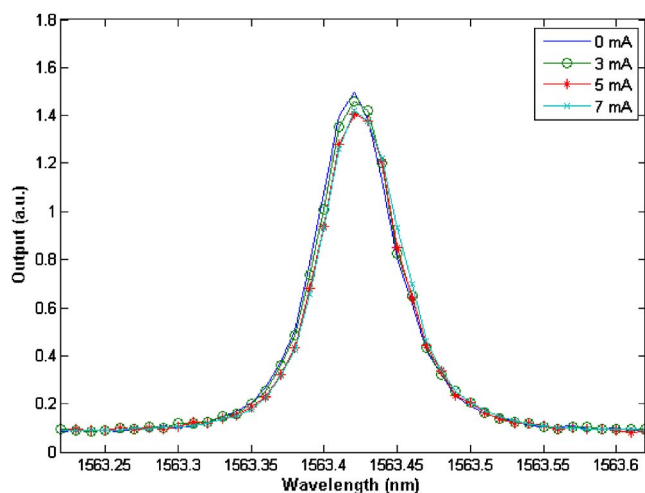


Fig. 10 Transmission spectrum of a MR with various heating currents sent to an adjacent microheater.

and input 4 and output 1 MR pairs tuned to λ_1 , λ_2 , λ_3 , and λ_4 , respectively. Given the different resonant wavelength peaks (at a fixed temperature) of the MRs and the different resistances of the microheaters, as listed in Table 1, the electric heating currents needed to tune the MRs to the chosen channel wavelengths have to be determined individually. To determine the heating current to tune a MR to λ_1 , for instance, the laser source was fixed at λ_1 , and then the heating current to the corresponding microheater was gradually increased until the MR reached resonance at λ_1 . Table 2 summarizes the heating currents required to tune the MRs to the corresponding wavelength channels, with the values in bold determined for the switching configuration described in Fig. 8.

The tuning response time of the device was evaluated by monitoring the output signal waveform of a MR with a high-speed photodetector (Thorlabs, DET 410), while modulating the heating current of the corresponding microheater with a square waveform. Similar tuning response time was observed for all eight MRs. Figure 9(a) and 9(b) illustrate the switch-on and switch-off time delay of a representative MR, respectively. The switch-on time is defined as the time required for the MR's output to reach 90% of the maximum output power after the heating current is turned on, which is close to 1 ms as observed in Fig. 9(a). A similar delay time of about 1 ms was observed for the MR switch-off time as shown in Fig. 9(b).

To evaluate the tuning thermal crosstalk between adjacent microheaters, we monitored the peak wavelength shift of one MR while heating up the microheater of an adjacent

MR. There was no peak wavelength shift observed even when a high heating current of 7 mA was provided to the adjacent microheater, as seen in Fig. 10. It should be noted that 7-mA heating current is sufficient to tune a MR by approximately 2.5 nm if supplied directly to the corresponding microheater. Therefore, the fabricated 4 × 4 photonic switch has no observable thermal crosstalk.

4 Conclusion

We have developed a tunable MR-based 4 × 4 photonic switch fabricated on a SOI substrate. Independent thermo-optic tuning of MRs was achieved with highly localized microheaters fabricated on the same substrate, yielding no crosstalk between adjacent MRs. The MRs have a FSR of about 18 nm, a FWHM of close to 0.1 nm, and a tuning response time of 1 ms. The independent MR tuning result suggests that the MRs may be fabricated with a reduced spacing to benefit the development of very large-scale integrated photonics.

Acknowledgment

This research was sponsored by the Missile Defense Agency and managed by the U.S. Army Space & Missile Defense Command.

References

1. B. E. Little, S. T. Chu, H. A. Haus, J. Foresi, and J.-P. Laine, "Microring resonator channel dropping filters," *J. Lightwave Technol.* **15**(6), 998–1005 (1997).
2. E. J. Klein, D. H. Geuzebroek, H. Kelderman, G. Sengo, N. Baker, and A. Driessen, "Reconfigurable optical add-drop multiplexer using microring resonators," *IEEE Photonics Technol. Lett.* **17**(11), 2358–2360 (2005).
3. R. Grover, T. A. Ibrahim, S. Kanakaraju, L. Lucas, L. C. Calhoun, and P.-T. Ho, "A tunable GaInAsP–InP optical microring notch filter," *IEEE Photonics Technol. Lett.* **16**(2), 467–469 (2004).
4. P. Dumon, W. Bogaerts, V. Wiaux, J. Wouters, S. Beckx, J. Van Campenhout, D. Taillaert, B. Luyssaert, P. Bienstman, D. Van Thourhout, and R. Baets, "Low-loss SOI photonic wires and ring resonators fabricated with deep UV lithography," *IEEE Photonics Technol. Lett.* **16**(5), 1328–1330 (2004).
5. A. Liu, R. Jones, L. Liao, D. Samara-Rubio, D. Rubin, O. Cohen, R. Nicolaescu, and M. Paniccia, "A high-speed silicon optical modulator based on a metal-oxide-semiconductor capacitor," *Nature (London)* **427**(6975), 615–618 (2004).
6. M. S. Nawrocka, T. Liu, X. Wang, and R. R. Panepucci, "Tunable silicon microring resonator with wide free spectral range," *Appl. Phys. Lett.* **89**(7), 071110–071113 (2006).
7. H. Y. Ng, M. R. Wang, D. Li, X. Wang, J. Martinez, R. R. Panepucci, and K. Pathak, "1 × 4 wavelength reconfigurable photonic switch using thermally tuned microring resonators fabricated on silicon substrate," *IEEE Photonics Technol. Lett.* **19**(9), 704–706 (2007).
8. Q. Xu, V. R. Almeida, and M. Lipson, "Micrometer-scale all-optical wavelength converter on silicon," *Opt. Lett.* **30**(20), 2733–2735 (2005).

Biographies and photographs of the authors not available.